X-ray and optical continua of active galactic nuclei with extreme Fe II emission

Mon. Not. R. Astron. Soc. **285**, 879–890 (1997)

X-ray and optical continua of active galactic nuclei with extreme Fe II emission

A. Lawrence,[1] M. Elvis,[2] B. J. Wilkes,[2] I. McHardy[3] and N. Brandt[4]

[1]*Institute for Astronomy, University of Edinburgh, Royal Observatory, Blackford Hill, Edinburgh EH9 3HJ*
[2]*Center for Astrophysics, 60 Garden Street, Cambridge MA 02138, USA*
[3]*Physics Department, Southampton University, University Road, Southampton SO9 5NH*
[4]*Institute of Astronomy, University of Cambridge, Madingley Road, Cambridge CB3 0HA*

Accepted 1996 October 25. Received 1996 October 23; in original form 1996 February 6

ABSTRACT

We present the results of *ROSAT* PSPC observations of three active galactic nuclei (AGN) with extremely strong Fe II emission (PHL 1092, IRAS 07598 + 6508 and I Zw 1) and two AGN with very weak Fe II emission (Mrk 10 and 110). The weak Fe II emitters have X-ray spectra typical of Type 1 AGN ($\alpha = 1.35$ and 1.41, where α is the spectral energy index). Of the strong Fe II emitters, two have steep spectra (PHL 1092 has $\alpha = 3.5$, and I Zw 1 has $= 2.0$) and the third, IRAS 07598 + 6508, is barely detected and so is extremely X-ray-quiet ($\alpha_{ox} = 2.45$). During our observations, PHL 1092 varied by a factor of 4, unusually fast for such a high-luminosity object, and requiring an efficiency of matter-to-energy conversion of 2 per cent or more. Compiling recently published data on other strong Fe II emitters, we find that they are *always* X-ray-quiet, and *usually* X-ray-steep.

Adding these data to the complete UVX-selected quasar sample of Laor et al., we find a statistical connection of Fe II/Hβ with α_x but not a simple relationship: weak Fe II emitters always have flat spectra, but strong Fe II emitters can be either flat or steep. A much cleaner relationship exists between Fe II strength and *X-ray loudness*, as quantified by α_{ix}, the spectral index between 1 μm and 2 keV. We also confirm that Fe II/Hβ anticorrelates with Balmer line velocity width, which in turn correlates well with both α_x and α_{ix} in the sense that AGN with narrow lines are X-ray-quiet. There is also marginal evidence that Fe II/Hβ correlates with both optical continuum slope and the curvature of the optical–UV–X-ray continuum: strong Fe II objects tend to have steeper continua and weaker 'blue bumps'. The amount of extinction required to explain the optical steepening compared to normal quasars [$E(B-V)$ in the range 0.2 to 0.6] suggests absorbing columns in the range $(1-3) \times 10^{21}$ cm^{-2}, just about the right amount to reduce the *ROSAT*-band X-ray flux by enough to explain the correlation with α_{ix}. However, the spectral shapes observed in the *ROSAT* band are not consistent with a simple absorption model.

Three objects in our total sample of 19 stand out persistently in all correlations: Mrk 231, IRAS 07598 + 6508 and Mrk 507. Interestingly, two out of the three are known to have low-ionization, broad absorption lines in the UV, and the third (Mrk 507) has no UV spectrum available. Furthermore, low-ionization, broad absorption lines are at least an order of magnitude more common in strong Fe II emitters than in quasars in general. Overall, *continuum shape* and *blueshifted absorption* should be added to the intriguing cluster of properties which all vary loosely together, and which has been isolated as 'eigenvector 1' by Boroson & Green: Fe II strength, velocity width, narrow-line strength and line asymmetry. We suggest that the underlying parameter is the density of an outflowing wind.

Key words: galaxies: active – galaxies: nuclei – quasars: emission lines – X-rays: galaxies.

1 INTRODUCTION

The Fe II emission lines which dominate the optical–UV spectra of many active galactic nuclei (AGN) have been seen as a worrying puzzle in two ways.

(i) Photoionization models have so far failed to replicate convincingly the strength of Fe II relative to the Balmer lines (see Joly 1993, and references therein). The solution to this problem may involve very high densities (e.g. Joly 1987), very large column densities (Collin-Souffrin, Hameury & Joly 1988; Ferland & Persson 1989), large iron abundance (Hamann & Ferland 1993), or indeed all of these. Almost certainly, non-photoionization heating is needed, but whether this requires only Compton and free–free heating from the overall AGN continuum (Collin-Souffrin et al. 1988; Ferland & Persson 1989) or, alternatively, implies additional non-radiative heating (Joly 1987, 1991, 1993) is not yet clear. Improved modelling of iron may also make a significant difference (Bautista & Pradhan 1995; see also Butler 1996, and references therein).

(ii) The relative strength of Fe II emission varies widely amongst different AGN, and shows intriguing correlations with other AGN properties: X-ray slope (Wilkes, Elvis & McHardy 1987), Balmer line velocity width (Wills 1982; Gaskell 1985; Zheng & O'Brien 1990; Zheng & Keel 1991; Boroson & Green 1992), narrow-line strength (Gaskell 1987; Boroson & Green 1992), radio loudness (Osterbrock 1977; Grandi & Osterbrock 1978; Bergeron & Kunth 1984) and, within radio-loud objects, core dominance (Joly 1991). Most of these correlations have been questioned, however (e.g. Boroson 1989; Zheng & O'Brien 1990), and are perhaps not simple dependencies but, rather, statistical tendencies. As they seem to be important clues to the AGN phenomenon, it is important to clarify their reality and nature.

Over the last decade several objects have been discovered which have 'superstrong' Fe II emission (Bergeron & Kunth 1980; Lawrence et al. 1988; Lipari, Macchetto & Golombek 1991). We quantify Fe II strength throughout this paper by the quantity $R_{\rm FeII}$ = Fe II 4570/Hβ, i.e., the relative fluxes in the 4570-Å feature (made up of transitions from multiplets 37 and 38) and in Hβ. Because standard photoionization models tend to have Fe II and Balmer lines tracking each other (e.g. Joly 1987), this is the most challenging quantity to test. Typical AGN have $R_{\rm FeII} \sim 0.4$, with 90 per cent of objects in the range 0.1 to 1.0. The extreme Fe II emitters have had claimed values of $R_{\rm FeII} \sim 4$–8, although the correct values are probably more like $R_{\rm FeII} \sim 2$–3 (see Section 4). These objects are obviously the hardest for photoionization models to explain, but also are important for testing the contentious correlations. Our main aim in this paper is to test the correlation with soft X-ray spectral shape. To do this, we made *ROSAT* PSPC observations, first of three very strong Fe II emitters (PHL 1092, IRAS 07598 + 6508 and I Zw 1), and secondly of two of the weakest known Fe II emitters, Mrk 10 and 110, based on the values of $R_{\rm FeII}$ quoted in the survey of Osterbrock (1977).

2 *ROSAT* OBSERVATIONS AND RESULTS

Observations were made using the X-Ray Telescope on board the *ROSAT* Observatory (Trümper 1983) with the Position Sensitive Proportional Counter (PSPC) (Pfeffermann et al. 1987) in the focal plane. The targets were placed on-axis, and a standard 400-s 'wobble' carried out in order to prevent shadowing behind the coarse-mesh grid covering the PSPC window. The dates and exposure times of the observations are summarized in Table 1. Of the five observations, four targets gave substantial count rates, but the fifth (IRAS 07598 + 6508) was barely detected.

The data for IRAS 07598 + 6508 were reduced and analysed using the Starlink ASTERIX package. The aspect was checked using positions of bright stars seen in the image, and confirmed the presence of a weak source at the position of IRAS 07598 + 6508 (Lawrence et al. 1988). We analysed the image using the point source searching routine (PSS). This does a sliding fit using an empirical point-spread function (PSF), which depends in turn on the PHA channels included. In the standard broad band, channels 11–240, we find 15.3 ± 5.4 counts. For the Galactic H I column in this direction, $N_{\rm H} = 4.3 \times 10^{20}$ cm^{-2}, we find that this corresponds to a monochromatic flux density at 1 keV of 3.8 ± 1.3 nJy.

The other four targets were reduced and analysed using the PROS package in IRAF. Source counts were extracted using a 3-arcmin aperture, and various background annuli, chosen to avoid nearby sources. Simple power-law model fits were made to the counts spectra using the 1993 January version of the detector response matrix. (We also tried using the 1992 March matrix, which made definite but fairly subtle differences.) The results are summarized in Table 2, and the spectra themselves and confidence contours for fitted parameters are shown in Figs 1 and 2.

Table 1. New X-ray observations.

name	z	date(s)	exposure	ROR	net counts
MKN 110	0.030	1-2/11/91 14-22/4/92	9390	700262	61993
MKN 10	0.030	17/3/91	4344	700261	4032
PHL 1092	0.396	19-22/92	7780	700259	2235
I Zw 1	0.061	31/12/91	3487	700260	2835
07598+6508	0.1483	17-18/3/91	8214	700258	15

Note. The exposure time is the actual exposure time at target position, not the elapsed time of observation.

Table 2. Results.

(1) Name	(2) Counts	(3) N_H(Gal)	(4) α_E	(5) N_H	(6) χ^2(dof)	(7) S_1
MKN 110	61993	20.08	1.41±0.03	20.15±0.02	94.9(28)	7160
(fix N_H=Gal)			1.41		95.0(29)	
MKN 10	4032	20.65	1.35±0.11	20.64±0.04	46.3(28)	2500
(fix N_H=Gal)			1.47		49.8(29)	
PHL 1092	2235	20.55	3.47±0.27	20.68±0.06	29.8(28)	150
(fix N_H=Gal)			3.05		36.9(29)	
I Zw 1	2835	20.71	2.03±0.14	20.83±0.03	24.1(28)	150
(fix N_H=Gal)			1.56		55.7(29)	
07598+6508	15.3±5.4	20.66				3.8±1.3

Notes. (a) All except IRAS 07598 + 6508 analysed with IRAF/PROS. All extracted with 3-arcmin aperture and various background annuli. Spectral fits performed on channels 3–34 inclusive. 'Jan 93' detector response matrix used throughout. (b) IRAS 07598 + 6508 analysed with ASTERIX/PSS. (c) N_H is $\log_{10}$ of column density, in units of atom cm^{-2} from Elvis et al. (1989) and Murphy et al. (1996). (d) S_1 is flux at 1 keV in nJy (in Earth frame).

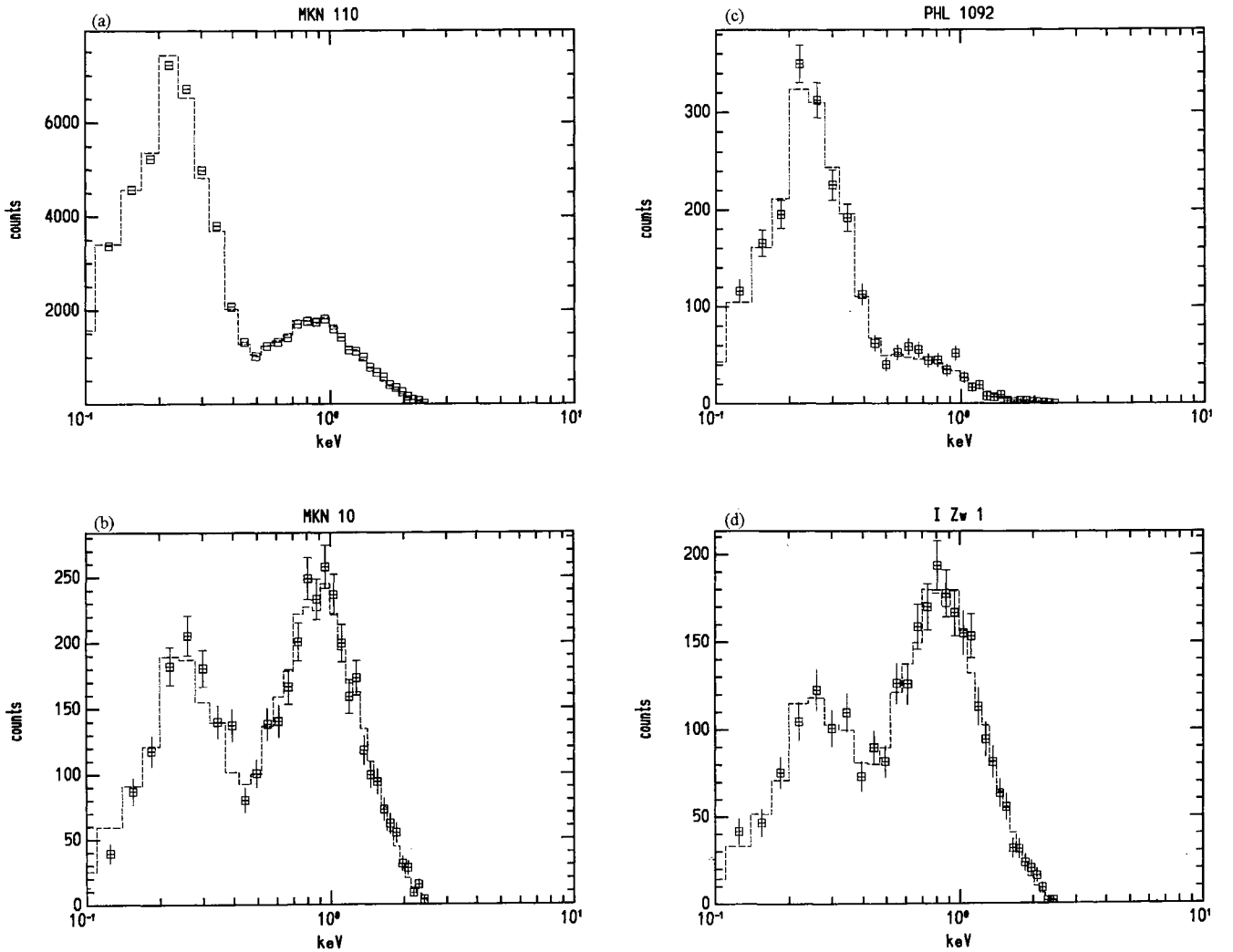

Figure 1. *ROSAT* X-ray count spectra. The error bars shown are 1σ statistical counting errors in each bin. The dashed line shows the expected count distribution from the best-fitting model tabulated in Table 2. (a) Mrk 110. (b) Mrk 10. (c) PHL 1092. (d) I Zw 1.

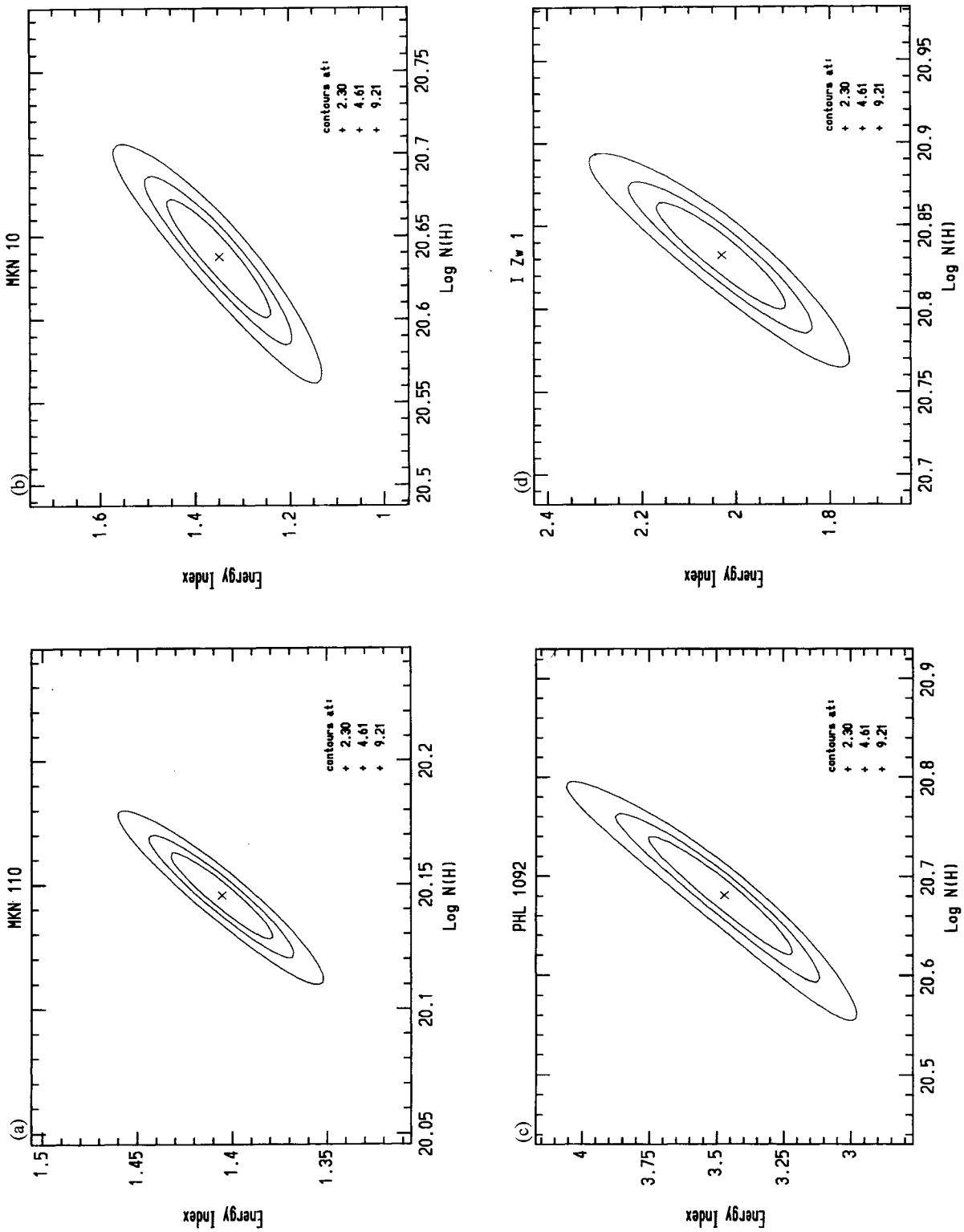

Figure 2. Confidence contours for the model fits to the spectra shown in Fig. 1. The contours shown trace models with the minimum value of χ^2 plus 2.30, 4.61 and 9.21 respectively. For two interesting parameters (i.e., the third parameter, normalization, has been allowed to find its best value in each case) these contours correspond to 68, 90 and 95 per cent confidence respectively. (a) Mrk 110. (b) Mrk 10. (c) PHL 1092. (d) I Zw 1.

2.1 Notes on *ROSAT* spectra of individual objects

Mrk 110. The spectral index found is quite typical for Type 1 AGN (e.g. Laor et al. 1994). The fitted H I column is consistent with the Galactic column in that direction. The formal quality of fit is poor, but this is misleading because of the huge number of counts and consequent small errors. The percentage deviations from the model are, in fact, much smaller than for the other three targets, which have formally more acceptable fits. The detector response matrix is simply not known well enough to test models at this level of accuracy. The observation was made at two quite distinct epochs, but there is no evidence for spectral change.

PHL 1092. This source was strongly variable during the observation. The variability is discussed in a little more detail in Section 2.2 below. The result in Table 2 is based on the total data. The fit is good, and shows an extremely steep spectrum, and a small excess column of $N_H = 1.1 \times 10^{20}$ cm^{-2}. [The implied reddening for Milky Way-like gas is small, $E(B-V) \sim 0.02$.] The galactic H I column is excluded at 95 per cent confidence, but not at 99 per cent.

I Zw 1. The fit is good, and shows a spectrum rather steeper than normal for Type 1 AGN ($\alpha = 2.03$), and a small excess column of $N_H = 1.7 \times 10^{20}$ cm^{-2}. [The implied reddening for Milky Way-like gas is small, $E(B-V) \sim 0.03$.] The Galactic H I column is excluded at better than 99 per cent confidence.

Mrk 10. The spectral index found is typical for Type 1 AGN, and the fitted column is consistent with the Galactic column. Formally, the fit is poor, and could be rejected at 95 per cent confidence. This might suggest that fitting a more complicated spectrum would be justified. However, there is no obvious pattern to the residuals, and this is one case where using the 1992 March matrix gave a better fit (reduced $\chi^2 = 1.25$) but exactly the same slope!

So far, then, it is noticeable that the two weak Fe II emitters (Mrk 10 and 110) have 'normal' X-ray spectra, whereas two out of three of the strong Fe II emitters have steep spectra, PHL 1092 extremely so. The third, IRAS 07598 + 6508, is very X-ray-quiet. In Section 4 we estimate that $\alpha_{ox} = 2.45$, compared to a more typical value for radio-quiet quasars of 1.5; in other words, the relative X-ray flux is 229 times weaker than average. (Here we define α_{ox} in the standard way as the logarithmic slope between 2500 Å and 2 keV.) Of course, it is quite possible that a large absorbing column is the cause of the faintness of the X-rays. Taking a standard interstellar absorption cross-section per hydrogen atom, we find that the column needed to reduce monochromatic X-rays at 1 keV by a factor of 229 is $N_H = 2.2 \times 10^{22}$ cm^{-2}.

2.2 Variability of PHL 1092

PHL 1092 was observed in six sections over 1992 January 19–22. The first observation was on January 19, and the other five grouped relatively closely together over January 21–22. The source increased in brightness by a large factor between the first and second observations; thereafter there is no significant variability. The January 19 observation has a count rate of 0.07 ± 0.01 count s^{-1}. The remaining five observations have mean count rate of 0.28 ± 0.01 count s^{-1}. Therefore the source showed an increase by a factor of 4 in 161 ks. We extracted a pulse-height distribution and fitted a spectrum to the low-state data. The fitted values (other than normalization) were indistinguishable from the mean spectrum. However, these data contain only about 100 counts, so the fitted errors are large. We cannot rule out a change in spectral index of the order of $\Delta\alpha \approx 1$, or a change in absorbing column of the order of $\Delta N_H \approx 4 \times 10^{20}$ cm^{-2}.

This degree of variability is unusual for an unbeamed object as luminous as PHL 1092. Because the spectrum is so steep, the total luminosity in the *ROSAT* band is very model-dependent, but is of the order 10^{39} W, assuming $H_0 = 50$ km s^{-1} Mpc^{-1} and $q_0 = 1/2$. A black hole massive enough to produce such a luminosity, if radiating at the Eddington limit, has $M = 8 \times 10^7$ M$_\odot$. The observed variability time-scale of 161 ks is much slower than the potential light-travel time at a few Schwarzschild radii, but is of a similar order to dynamical time-scales. For example, with the mass above, at $R = 3R_S$ the orbital time-scale is roughly 35 ks. If the black hole is radiating at a fraction of the Eddington limit, the dynamical time-scale is proportionally longer, and so real physical models may be tightly constrained by such variability. The implied limit on the efficiency of energy generation is also interesting; given $\Delta L \sim 3/4 \times 10^{39}$ W and $\Delta t = 161$ ks, we find $\eta \geq 2$ per cent, inconsistent with energy generation by nuclear fusion. It is hard to believe that, for instance, a starburst model could produce this efficiency.

It is also interesting to make empirical comparisons. From the studies of Green, McHardy & Lehto (1993) and Lawrence & Papadakis (1993) we can see that large changes (of order unity) at such high luminosities occur typically on time-scales of months or longer, so that the event we have seen is unusually fast and/or large. On the other hand, Barr & Mushotzky (1986) compiled the *fastest* observed doubling time-scales for AGN; at $L_x \sim 10^{39}$ W this of the order 10^5 s. So the event we have seen, while unusual, is not unprecedented. Boller, Brandt & Fink (1996) have suggested that X-ray variability in narrow-line AGN (of which PHL 1092 is an example) is systematically larger and/or faster than in AGN in general; a particularly impressive example is seen in IRAS 13224 − 3809 (Boller et al. 1993). The event we have seen here then adds more weight to that claimed effect.

3 *ROSAT* RESULTS FOR OTHER STRONG Fe II EMITTERS

ROSAT PSPC spectral information has been published for four other superstrong ($R_{Fe\,II} > 2$) Fe II emitters: Mrk 231, IRAS 13224 − 3809, 5C 3.100 and Mrk 507. We discuss these in turn.

Mrk 231. An X-ray spectrum has been published by Rigopoulou, Lawrence & Rowan-Robinson (1996) as part of a study of the radio to X-ray energy distributions of ultraluminous *IRAS* galaxies. A power-law model fit to a count spectrum with 363 counts found $\alpha = 1.14 \pm 0.27$, actually rather flatter than normal for a Type 1 AGN. The fit quality was very bad, however. An improved but still not very good fit was found by adding an emission feature at 0.88 keV. The 1-keV flux found was only 30.9 nJy, much fainter than other bright local AGN. Overall then, Mrk 231 does not have a steep spectrum, but is X-ray-quiet. (This will be quantified in Section 4.)

IRAS 13224−3809. This object was found in the cross-correlation of the *ROSAT* All-Sky Survey with the *IRAS* catalogue by Boller et al. (1992), who show it to be a high-luminosity AGN with a very steep spectrum. Follow-up optical spectroscopy by Boller et al. (1993) shows that it has both extremely strong Fe II emission, $R_{\rm Fe\,II}=2.4$, and very narrow lines. The pointed *ROSAT* observation in the same paper finds a spectrum with $\alpha=3.4\pm0.2$ and a 1-keV flux of 609 nJy. (No error on the flux is given by Boller et al.)

5C 3.100. A *ROSAT* spectrum has been published in a study by Boller et al. (1996) of Type 1 AGN with narrow lines. They find a moderately steep spectrum, $\alpha=1.9\pm0.2$.

Mrk 507. This object is also in the study by Boller et al. (1996). They find a flat spectrum, $\alpha=0.6\pm0.3$.

Finally, we comment on the interesting case of 3C 351. The status of this object as a strong Fe II emitter is not clear. Grandi (1981) found $R_{\rm Fe\,II}=1.63$, but Boroson & Green (1992) found no significant detection of Fe II emission. New optical data taken by one of us (BW) confirms the weakness of Fe II emission. Next, we note that 3C 351 is in the 'ultra-soft sources' sample of Cordova et al. (1992). Fiore et al. (1993) report a *ROSAT* observation, for which they find that the object is X-ray-quiet by radio-loud AGN standards, though not extremely so by radio-quiet AGN standards. A standard power-law fit gives $\alpha=0.47\pm0.16$, i.e., extremely flat, but the fit quality is unacceptable; the spectrum is clearly complex. Fiore et al. consider various alternatives, most of which imply a considerably steeper underlying power law – for example, a partial covering model gives $\alpha=2.12\pm0.04$. Their preferred model involves a warm absorber between us and the central X-ray source. Because of the uncertainty over both the Fe II emission and the X-ray spectrum, we will not consider this object further.

4 CORRELATIONS BETWEEN X-RAY AND OPTICAL PROPERTIES

Our main aim is to test the correlation of X-ray spectral index with Fe II strength. Because it has become clear that AGN spectra are steeper in the *ROSAT* band than in the *Einstein* IPC band (e.g. Laor et al. 1994), we should use only *ROSAT* spectra. One limitation of earlier studies has been the large uncertainty in X-ray spectral index. It is therefore important to use high-quality spectra. In the *ROSAT* band, this means using objects with low column density, in order to minimize systematic errors, as well as using observations with a large number of counts. We therefore use the sample of Laor et al. (1994), whose objects are from a redshift- and Galactic column density-limited subset of a complete optically selected sample, and which all have high-quality X-ray spectra. To this sample we add the objects reported in this paper, plus the four other strong Fe II emitters with reasonable *ROSAT* information (see Section 3). For the Laor et al. sample, we use the $R_{\rm Fe\,II}$ values in table 5 of Laor et al. (1994). For the other objects we use a variety of sources, as summarized in Table 3. In particular, some data are from

Table 3. Summary data.

(1) name	(2) R(FeII)	(3) α_x	(4) α_{ox}	(5) α_{ix}	(6) α_{io}	(7) FWHM
MKN 10	0.31 (1) <0.11 (2)	1.35±0.11 (1)	1.19	1.20	1.24	2790 (1)
MKN 110	0.14 (3) 0.09 (2) 0.16 (4)	1.41±0.03 (1)	1.08	1.14	1.40	2120 (3)
PHL 1092	1.81 (1) 6.20 (5)	3.47±0.27 (1)	1.55	1.33	0.37	1300 (5)
I Zw 1	1.47 (3) 1.34 (4)	2.03±0.14 (1)	1.41	1.42	1.46	1240 (3)
07598+6508	2.60 (1) 2.30 (6) 4-8 (8)	--	2.45	2.16	0.90	2900 (6) 2550 (7)
MKN 231	2.03 (6) 1.36 (4)	1.14±0.27 (9)	1.76	1.97	2.88	3000 (10) 2870 (7) 3000 (11)
13224-3809	2.40 (12)	3.40±0.20 (12)	1.52	1.42	0.99	650 (12)
5C 3.100	2.70 (13)	1.90±0.20 (13)	1.31	1.46	2.11	685 (13)
MKN 507	2.70 (13)	0.60±0.30 (13)	1.36	1.64	2.86	960 (13)

Notes. (a) Where more than one value is noted, the first one is the one used in correlations. (b) R(Fe II) = Fe II/Hβ refers to relative strength of the 4570-Å feature. (c) α_x is *ROSAT* energy index. (d) α_{ox} and α_{ix} are power-law slopes from 2 keV to 2500 Å and μm respectively, in source frame (for derivations see text).

References. (1) This paper. (2) Osterbrock (1977). (3) Boroson & Green (1992). (4) Joly (1991, and references therein). (5) Bergeron & Kunth (1984). (6) Lipari (1994). (7) Boroson & Meyers (1992). (8) Lawrence et al. (1988). (9) Rigopoulou et al. (1995). (10) Lipari et al. (1993). (11) Lipari et al. (1994). (12) Boller et al. (1993). (13) Boller et al. (1996, and references therein).

our own optical spectroscopy. All five of our *ROSAT* targets were observed using the MMT red spectrograph, at 20-Å resolution, with exposures typically of the order of a few hundred seconds. Mrk 10 and 110 were observed in 1991 May; the other targets were observed in 1991 September. All observations were photometric. However, we use higher resolution data from the literature where they are available. A summary of values of α_x and $R_{\rm Fe\,II}$ is given in Table 3. Note that there is considerable variation in the reported Fe II strengths. Quantifying Fe II is a very difficult problem, because of the uncertainty in the continuum level, the extreme (and linewidth- and resolution-dependent) blending of the Fe II transitions, and because of the blending of Hβ with Fe II multiplets 30 and 42. We therefore prefer estimates based on fitting a model of the Fe II and Balmer line spectrum. We do not quote formal errors on $R_{\rm Fe\,II}$, as the real uncertainties are dominated by the problems described above, but the reader should bear in mind that the errors are always of the order 20–30 per cent or even worse.

Given the tendency we have already noted for strong Fe II emitters to be X-ray-quiet, we also collect optical/UV continuum data in order to estimate a value for α_{ox}. Furthermore, it was clear from inspection of published spectra and photometry that the strong Fe II emitters quite often have steeper optical spectra than quasars in general. (Typical UVX-selected quasars have $\alpha_{opt} \sim 0.2$ whereas, as we shall see, strong Fe II emitters have $\alpha_{opt} \sim 1$ or more.) It is not clear whether the steepening is intrinsic or due to reddening, but in either case it seemed wise also to characterize X-ray loudness by the spectral index between 1 μm and 2 keV, which we call α_{ix}. We therefore collected fluxes at 2 keV, 2500 Å and 1 μm, in the rest-frame of the object. In all cases we estimated the 2-keV flux from the spectral parameters of the *ROSAT* PSPC spectral fits. The flux at 2500 Å was estimated in most cases from the *IUE* ULDA archive data, and in other cases extrapolated from optical photometry. The 1-μm flux was estimated by interpolation of optical/IR photometry collected from the catalogues of Gezari, Schmitz & Mead (1987) and Véron-Cetty & Véron (1989, hereafter VCV), except where noted below. Note that although these objects are very likely to be variable, and the measurements we use are not contemporaneous, the quantity α_{ix} is relatively insensitive to this problem; a factor 2 variation at one wavelength and not the other changes the index by only 0.09.

Some authors (e.g. Zheng & O'Brien 1990; Boroson & Green 1992) have suggested that Fe II strength correlates better with Hβ FWHM than with X-ray spectral index. We therefore have also collected data on linewidths. The data used are summarized in Table 3. Below we give some notes on individual objects, and then proceed to analyse the correlations.

4.1 Notes on individual objects

Mrk 10. This object was selected for *ROSAT* observation because of the very low $R_{\rm Fe\,II} < 0.11$. Our own spectroscopy shows rather stronger but still weak Fe II. The strength of the 4570-Å feature was estimated by fitting a linear continuum between Hβ and Hγ.

Mrk 110. This object was also selected for *ROSAT* observation because of the very low $R_{\rm Fe\,II}$ value listed by Osterbrock (1977), $R_{\rm Fe\,II} = 0.09$. Other quoted values are roughly consistent. We note a difference of a factor 3 between the *UBV* photometry of VCV, and the spectrophotometry of Boroson & Green, and we use the former, extrapolating to 1 μm.

PHL 1092. The Fe II strength was kindly estimated for us by T. Boroson, who fitted his Fe II model spectrum to our spectroscopic data. The result is a value of $R_{\rm Fe\,II}$ that is very much smaller than the Bergeron & Kunth (1980) measurement. The main reason for this difference is that Bergeron & Kunth suggested that most of the feature at ~ 4860 Å is actually due to Fe II multiplet 42, whereas we find that it is roughly half Hβ. No *IUE* spectrum is available but, given the large redshift, the extrapolation to 2500 Å from the *U*-band photometry is modest.

I Zw 1. The various Fe II strengths agree reasonably.

IRAS 07598 + 6508. Lipari (1994) finds that this object is a broad-absorption-line QSO (BALQSO) as well as having very strong Fe II emission. The Fe II strength was kindly estimated for us by T. Boroson, who fitted his Fe II model spectrum to our spectroscopic data. The result is a value of $R_{\rm Fe\,II}$ that is very much smaller than the Lawrence et al. (1988) measurement, but in reasonable agreement with the value of Lipari (1994). As with PHL1092, the main reason for the discrepancy is probably the relative contributions of Hβ and the emission from Fe II multiplet 42. No *J*-band photometry is available; we have extrapolated from the spectrophotometry of Lipari (1994), which is in good agreement with the *B*-band magnitude of Lawrence et al. (1988).

Mrk 231. This well-known object is also a BALQSO (Boksenberg et al. 1977; Lipari et al. 1994), which makes the emission-line properties particularly hard to model. We choose the more recent estimate.

IRAS 13224 − 3809. The only photometry available is the spectrophotometry of Boller et al. (1993). We have extrapolated to 2500 Å as a power-law using those data.

5C 3.100. Also known as Mrk 957. We have used the recent UV spectroscopy by Gaskell & Koratkar (1996) and the *UBV* photometry by VCV, as the spectrum given by Halpern is only very poor photometry (Halpern, private communication). The IR photometry of Lawrence et al. (1985) is in reasonable agreement with VCV. The UV spectrum of this object shows no emission lines, and Gaskell & Koratkar (1996) suggest that it may be a BAL object; however, the spectrum is too noisy to come to a conclusion.

Mrk 507. Again we choose not to use the spectrum of Halpern & Oke (1987), and instead use the VCV photometry. No *IUE* or *J*-band photometry is available, so we have extrapolated using the VCV photometry.

4.2 Correlation results

Figs 3–5 show correlation results.In each figure we also indicate the significance of any possible correlation using Spearman's rank correlation coefficient *r*. For the given value of *r* we show the probability of achieving a value either greater than *r* or less than $-r$ for randomly selected ranking, i.e., we have used a two-tailed test of significance. A persistent group of objects (Mrk 231, IRAS 07598 + 6508 and Mrk 507) were found to be outliers. We therefore

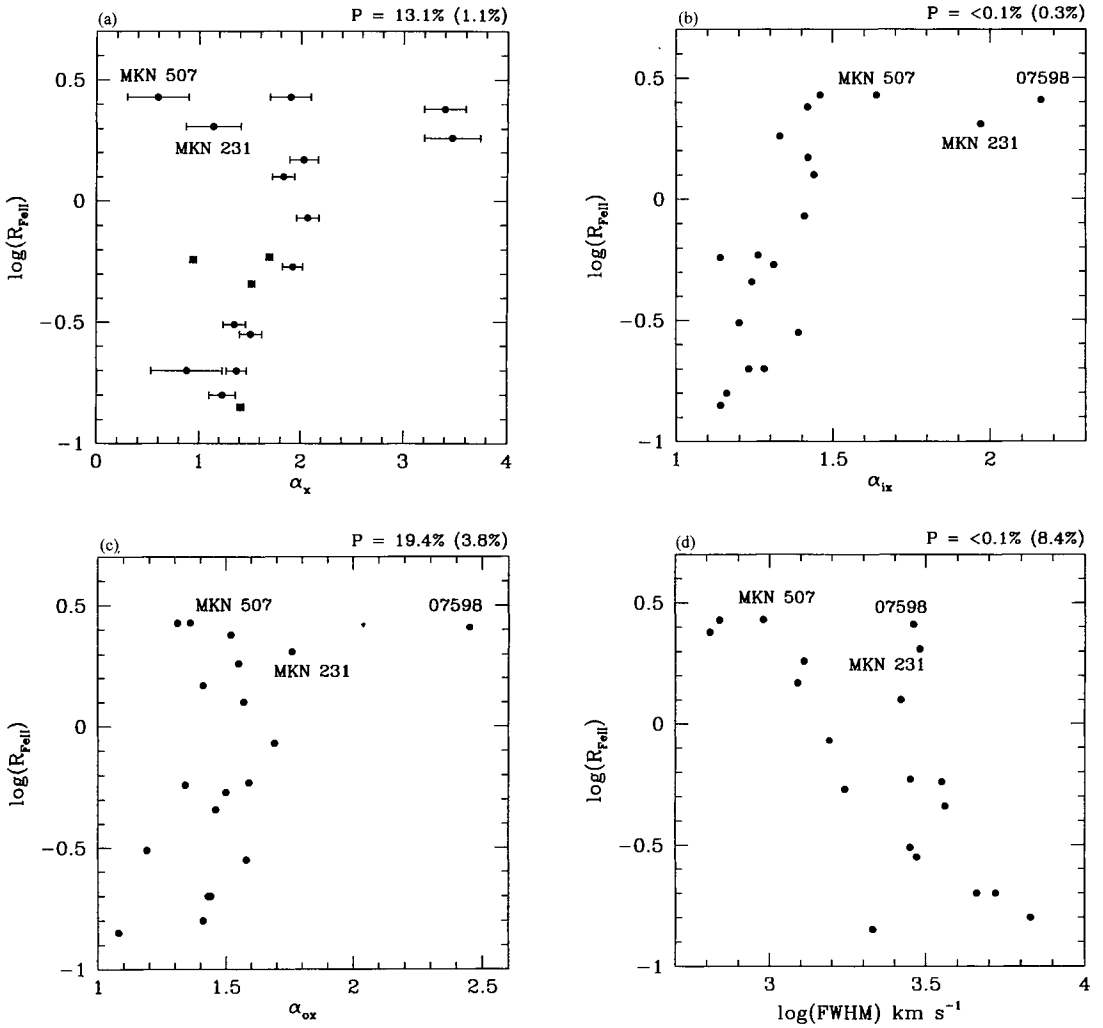

Figure 3. Relationship between $R_{Fe\,II}$ and (a) X-ray spectral index α_x, (b) X-ray loudness as expressed by α_{ix}, (c) X-ray loudness as expressed by α_{ox}, and (d) emission-line FWHM. In each case the percentage given at top right represents the significance of the correlation according to a two-tailed rank-correlation test. The number in brackets is the significance after excluding IRAS 07598 + 6508, Mrk 231 and Mrk 507.

repeated the significance test in each case excluding these objects. (The results are shown in brackets.) Note that we have *not* excluded a different list of selected objects from each correlation; rather we have removed the *same* list of three from all correlations.

In Fig. 3(a) we show the resulting correlation between $R_{Fe\,II}$ and α_x. The *statistical connection* looks reasonable by eye, but is only marginally significant. The evidence for a *direct relationship* is even weaker. Either Mrk 507 and 231 are exceptions for some reason (note that IRAS 07598 + 6508 is not included in this plot, as it has no X-ray spectrum), or one has to accept that the relationship is only a probabilistic one: weak Fe II emitters always have flat soft X-ray spectra, but strong Fe II emitters can have either flat or steep spectra. A much better and clearly significant correlation is seen between α_{ix} and Fe II strength (Fig. 3b). Mrk 231 and IRAS 07598 + 6508 stand out from the trend, but in a direction that strengthens the qualitative statement that strong Fe II emitters are consistently X-ray-quiet. The same effect is probably present in α_{ox} (Fig. 3c), but the scatter is noticeably larger, and the correlation less significant. Mrk 231 is now consistent with the trend, but only accidentally; it has a particularly steeply falling optical/UV spectrum, which lowers α_{ox} for a given α_{ix}. Finally, Fig. 3(d) confirms the anticorrelation between $R_{Fe\,II}$ and Balmer line FWHM previously seen by Wills (1982), Gaskell (1985), Zheng & O'Brien (1990), Zheng & Keel (1991) and Boroson & Green (1992).

Next, we look at further linewidth correlations. Fig. 4(a) shows that FWHM anticorrelates with X-ray spectral index, as claimed by Laor et al. (1994) and Boller et al. (1996). The clear outliers here are Mrk 231 and 507. As with the $R_{Fe\,II}$ versus α_x correlation, either one believes that these two objects are exceptions for some reason, or one accepts a probabilistic connection rather than a direct relationship. Next, Fig. 4(b) shows a correlation between FWHM and α_{ix}. Once again, Mrk 231 and IRAS 07598 + 6508 stand out. Finally, Fig. 4(c) shows FWHM versus α_{ox}, which shows no correlation at all. It is interesting that both Fe II strength and Balmer line velocity width seem to be more closely connected to α_{ix} than to α_{ox}. This could be because α_{ox} has some extra 'noise' on it, such as small but variable amounts

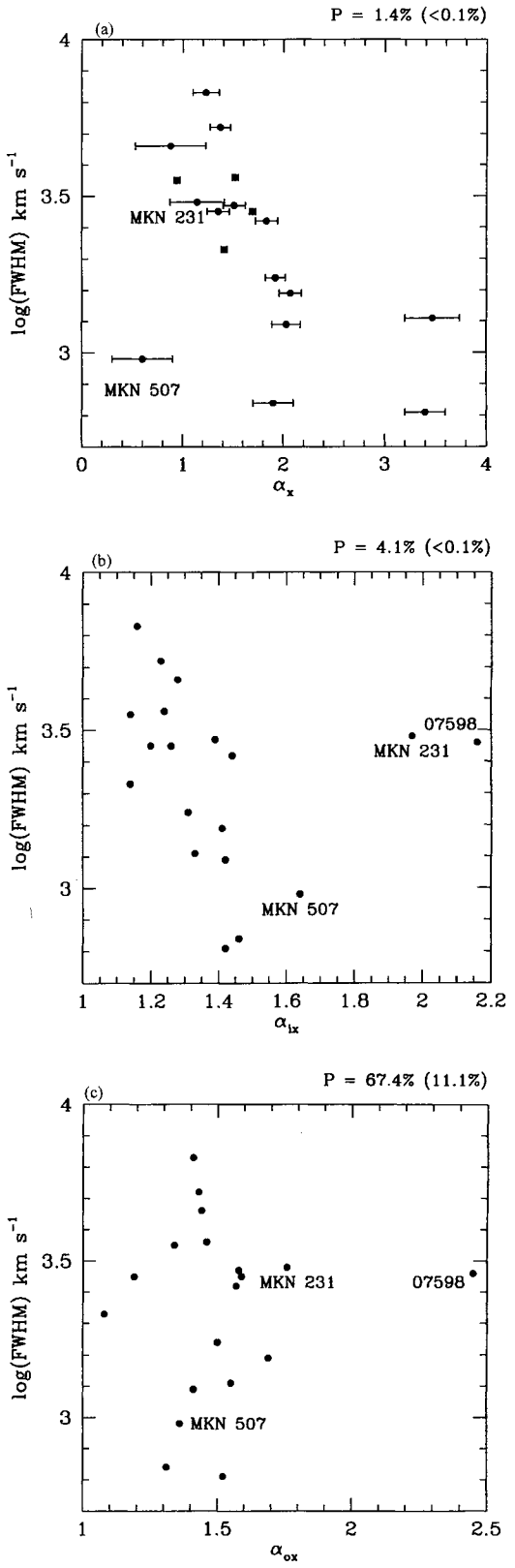

Figure 4. Relationship between emission line FWHM and (a) X-ray spectral index α_x, (b) X-ray loudness as expressed by α_{ix}, and (c) X-ray loudness as expressed by α_{ox}. In each case the percentage given at top right represents the significance of the correlation according to a two-tailed rank-correlation test. The number in brackets is the significance after excluding IRAS 07598 + 6508, Mrk 231 and Mrk 507.

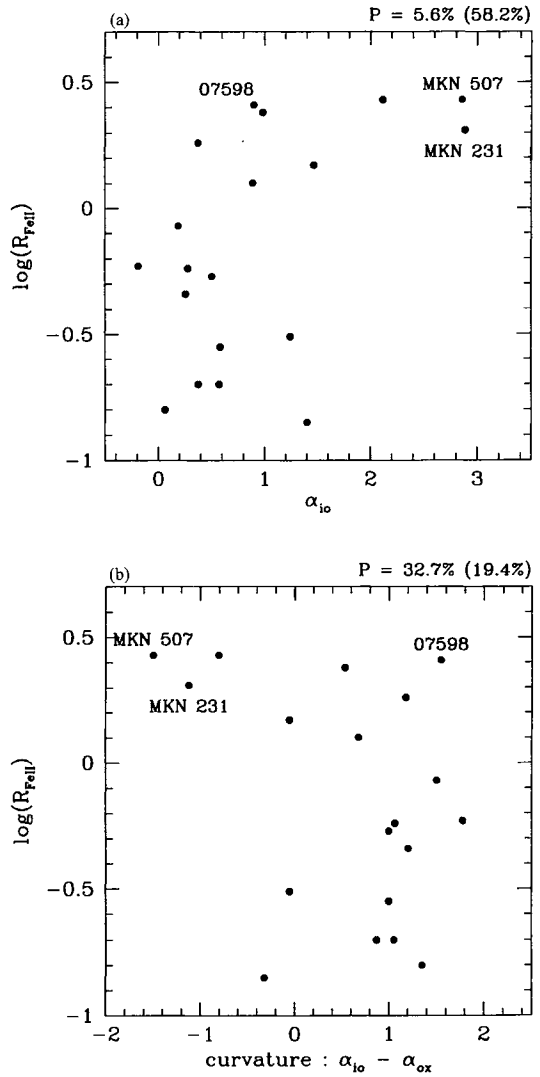

Figure 5. Relationship between $R_{Fe\,II}$ and (a) optical continuum shape, α_{io}, and (b) continuum curvature, as expressed by $\alpha_{ox} - \alpha_{io}$. In each case the percentage given at top right represents the significance of the correlation according to a two-tailed rank-correlation test. The number in brackets is the significance after excluding IRAS 07598 + 6508, Mrk 231 and Mrk 507.

of line-of-sight reddening, or it could mean that overall X-ray loudness is the prime variable, rather than blue-bump strength.

Finally, we examine two more possible correlations which clarify the relationship between Fe II strength and continuum shape. Fig. 5(a) shows marginal evidence that $R_{Fe\,II}$ also correlates with α_{io}, the slope between the near-infrared and the UV. Objects with weak Fe II have optical slopes which are flat or only slightly falling, corresponding to the rise of the 'blue bump', whereas strong Fe II emitters are steeply falling throughout the optical, UV, and X-ray. Fig. 5(b) shows the curvature of the spectrum, estimated as $\alpha_{io} - \alpha_{ox}$. The scatter is very large, and there is not a significant correlation, but it seems that weak Fe II emitters typically have positive values, reflecting the convex shape of the blue bump, whereas strong Fe II emitters are either consistent

with a single power law or actually concave. Strong Fe II emitters are therefore both X-ray-quiet and have weak blue bumps.

4.3 Broad-absorption-line connection

Along with the fascinating correlations discussed so far, another interesting connection emerges. It has been suggested that BALQSOs have stronger than average Fe II emission (Hartig & Baldwin 1986; Weymann et al. 1991). We can confirm the same connection in reverse. Two out of seven of our extreme Fe II emitters, Mrk 231 and IRAS 07598 + 6508, are BALQSOs, compared to 9 per cent in the optically selected quasar population. More strikingly, they are both *low-ionization* BALQSOs, which constitute only 1.5 per cent of the optically selected quasar population (Weymann et al. 1991). The key Mg II feature is in the UV, and only four of our sample have such data, so the presence of the BAL phenomenon could be even more widespread. (Gaskell & Koratkar 1996 present some evidence that 5C 3.100 may also be a BAL object, but their UV spectrum is too noisy to provide a conclusive result.) A connection between Fe II strength and blueshifted absorption is also evident from the work of Low et al. (1989) and Boroson & Meyers (1992), who studied the spectra of IR-selected QSOs and have found them both to have stronger than normal Fe II emission and a much enhanced probability of low-ionization broad absorption lines.

As well as the intrinsic interest of a connection between absorption lines and Fe II strength, there is a potential for *cleaning up* the correlations that we have examined. Three objects stand out away from the trends, in the sense of being too X-ray-quiet and/or having too flat X-ray spectra: Mrk 231, IRAS 07598 + 6508 and Mrk 507. Two out of these three are absorption-line objects, and the third (Mrk 507) has no UV data. It is highly likely, then, that these objects suffer from soft X-ray absorption by ionized gas, which would not be easily recognized by the standard spectral fits. As well as reducing the overall soft X-ray flux, the fitted power-law spectral index may not be meaningful. We note that the object we excluded from our sample, 3C 351, also has blueshifted UV absorption lines and an apparently flat X-ray spectrum, which is actually much better fitted with a warm absorber model and steeper underlying spectrum (Fiore et al. 1993; their simple power-law fits give $\alpha = 0.5 \pm 0.2$, wheres the warm absorber gives $\alpha = 1.0 \pm 0.2$). Indeed, Mathur et al. (1994) show that a consistent model can be made with UV and X-ray absorption by the *same* ionized gas.

4.4 Role of reddening

The optical steepening seen in strong Fe II emitters suggests the possibility of extinction by dust. The steepening seen is $\Delta\alpha_{io} \sim 1$–2.5, corresponding to a reduction of flux at 2500 Å compared to 1 μm from a factor 4 to a factor 30. Assuming a standard Milky Way extinction law, this in turn correpsonds to $E(B-V)$ in the range 0.2 to 0.6. This is consistent with the kind of narrow-line reddenings deduced by De Zotti & Gaskell (1985). What effect would this material have on the X-ray flux in the *ROSAT* band? Again assuming a typical Milky Way gas-to-dust ratio, the absorbing columns would be in the range $(1$–$3) \times 10^{21}$ cm^{-2}. At 0.5 keV such columns would produce a change in monochromatic flux density ranging from roughly a factor 2 to roughly a factor 10. This would produce a steepening of the order $\Delta\alpha_{ix} \sim 0.1$–$0.4$, which is just about the right amount to explain the bulk of the α_{ix} trend (but not the two most extreme cases, Mrk 231 and IRAS 07598 + 6508, which require an order of magnitude more absorption). However, simple absorbing columns of the order $(1$–$3) \times 10^{21}$ cm^{-2} are very clearly excluded by the spectra actually seen in the *ROSAT* band, which suggest that any absorption is an order of magnitude smaller. We therefore have a kind of spectral paradox, where simple absorption adequately explains the gross IR–optical–X-ray energy distribution, but not the local X-ray spectrum.

Hard X-ray observations of strong Fe II emitters are clearly very desirable to resolve this conundrum. Meanwhile, interesting possibilities that should be explored include (a) two components to the X-ray spectrum, with differential absorption, and (b) absorption by ionized gas.

5 DISCUSSION

A number of consistent correlations amongst quasar properties have been emerging from the literature. In particular, Boroson & Green (1992) made a comprehensive study of the optical spectra of PG quasars, and performed a principal components analysis. They did not find a nice clean 'fundamental plane': five eigenvectors were required to account for the first 3/4 of the observed variance. However, their largest single eigenvector ('eigenvector 1', which contained ~ 30 per cent of the variance) was very close to being parallel to various measures of Fe II strength, and was also anticorrelated with [O III] strength and with Hβ FWHM, and positively correlated with blue asymmetry in the Hβ line. The second eigenvector was dominated by optical luminosity, although this also has a significant component along eigenvector 1. X-ray loudness, as expressed by α_{ox}, seemed to be weakly connected to both eigenvectors 1 and 2. Next, there is the claimed correlation between Fe II strength and X-ray spectral index (Wilkes, Elvis & McHardy 1987). We have confirmed such a correlation in this paper by considering the most extreme objects, and have also suggested that there is an even better correlation with X-ray loudness, and that this is better quantified as α_{ix} than as α_{ox}. Next, Laor et al. (1994) have claimed an anticorrelation between X-ray spectral index and Hβ FWHM. Such a connection is implicit in the observation that AGN selected to have steep soft X-ray spectra tend to have narrow lines (Puchnarewicz et al. 1992), and in the observation that AGN selected to have narrow lines tend to have steep soft X-ray spectra (Boller et al. 1996). We have confirmed the correlation here, and further shown that linewidth anticorrelates with X-ray loudness. Once again, α_{ix} seems more closely connected than the traditional α_{ox}. Finally, Joly (1991) has claimed that amongst radio-loud objects, Fe II strength is positively correlated with core dominance.

As well as confirming many of the above correlations, we have shown in this paper that Fe II strength and linewidth seem to be most closely connected with *continuum shape* in general. Strong Fe II emitters have steeper optical spectra, are more X-ray-quiet, have steeper X-ray spectra and have

weaker blue bumps. Summarizing our results and those listed above, objects with strong Fe II emission tend to have weak and steep X-ray emission, large overall luminosity, weak blue bumps, weak [O III], narrow and blue-asymmetric permitted lines, absorption features from outflowing ionized material and, in radio-loud objects, stronger core radio emission. Finally, although no direct correlation of variability with Fe II strength has been shown, it is clear that narrow-lined AGN have quite dramatic X-ray variability (Boller et al. 1996). Table 4 summarizes all these somewhat confusing trends.

Boroson & Green (1992) argued that viewing angle is unlikely to be the explanation of their 'eigenvector 1', because [O III] is likely to be isotropic, being optically thin and coming from large radii. However, it is possible that a large fraction of [O III] emission may come from a small enough radius to be obscured by the molecular torus needed in AGN unification schemes. This then implies that weak O III emitters, and thus strong Fe II emitters, are seen edge-on, inconsistent with the otherwise attractive idea that low-ionization lines come from the surface of a disc. Likewise, narrow lines would come from a face-on disc, but it is difficult to see how such objects would have preferentially weaker O III emission. More generally, Fe II and Hβ are very unlikely to have such very different degrees of anisotropy, whatever the geometry.

A direct causal connection with ionizing continuum shape seems initially attractive. In the standard photoionization models, hard X-rays heat the extended ionized zone, so one might expect more overall Fe II emission, but the temperature will be higher, which would decrease Fe II with respect to Hβ (Joly 1987). However, in absolute terms, the standard photionization models would make it very hard to explain the large values of $R_{\rm Fe\,II}$ seen in even moderately strong Fe II emitters, although this failure of photoionization models may change with improved atomic modelling, as discussed in the introduction.

Another route out of this dilemma is to argue that the low-excitation part at least of the BLR comes from gas that is mechanically rather than radiatively heated (Joly 1987,1991, 1993). The value of $R_{\rm Fe\,II}$ then depends strongly on density (Joly 1987, 1993). Given the connection of Fe II strength with the presence of low-ionization, blueshifted broad absorption lines, and with blue-asymmetric emission lines, which suggests radial outflow together with obscuration, this suggests that the parameter underlying 'eigenvector 1' is the *density of an outflowing wind*, in which broad-line clouds are comoving condensations. To go any further would require a proper model, but it seems quite reasonable at least that for given kinetic and ionizing luminosities, a denser wind would mean (i) a smaller outflow velocity, (ii) a lower ionization parameter, (iii) a larger optical depth in both dust and gas, leading to continuum steepening, (iv) stronger Fe II, and (v) possibly brighter radio emission through increased shock dissipation and consequent particle acceleration. Norman & Miley (1984) suggested a more specific scenario of this kind, in which low-excitation lines in radio-loud objects come from the interaction of a jet with its environment. They further suggested that the two fundamental parameters underlying a wide range of AGN types are *jet power* and *density of the environment*. On the other hand, Lipari (1994) and Lipari et al. (1994) discuss the idea of a 'superwind' in the context of starburst models of BALQSOs. These are both appealing schemes, but the general idea of outflow and mechanical dissipation could be of potential importance in a wider range of models.

Table 4. Qualitative summary of quasar correlations.

FeII	strong	==========>	weak
X-ray spectrum	steep	==========>	flat
X-ray flux	weak	==========>	strong
Blue Bump	weak	==========>	strong
BLR width	narrow	==========>	broad
BLR asymmetry	blue	==========>	none or red
OIII strength	weak	==========>	strong
Luminosity	high	==========>	low
Variability	high	==========>	low

6 CONCLUSIONS

Observations of AGN with extreme values of Fe II strength, and high-quality X-ray spectra, have clarified several correlations which have seemed ambiguous and confusing for some time. A fascinating cluster of properties linking dynamics (linewidths), dissipation of energy (Fe II strength) and radiation processes and/or absorption (continuum shape) seems to be emerging. The situation is still far from clear, however, and no proposed explanation is convincing thus far. It seems hard to resist the feeling that nature is telling us something important here, but we do not yet know what it is.

REFERENCES

Barr P., Mushotzky R. F., 1986, Nat, 320, 421
Bautista M. A., Pradhan A. K., 1995, J. Phys. B, B28, L171
Bergeron J., Kunth D., 1980, A&A, 85, L11
Bergeron J., Kunth D., 1984, MNRAS, 207, 263
Boksenberg A., Carswell R., Allen D., Fosbury R., Penston M., Sargent W., 1977, MNRAS, 178, 451
Boller Th., Meurs E. J. A., Brinkmann W., Fink H., Zimmermann U., Adorf H.-M., 1992, A&A, 261, 57
Boller Th., Trümper J, Molendi S., Fink H., Schaeidt S., Caulet A., Dennefeld M., 1993, A&A, 279, 53
Boller Th., Brandt W. N., Fink H., 1996, A&A, 305, 53
Boroson T.A., 1989, ApJ, 343, L9
Boroson T. A., Green R. F., 1992, ApJS, 80, 109
Boroson T. A., Meyers K. A., 1992, ApJ, 397, 492
Butler K., 1996, Phys. Scripta, T65, 63
Collin-Souffrin S., Hameury J. M., Joly M., 1988, A&A, 205, 19
Cordova F. A., Kartje J. F., Thompson R. J., Mason K. O., Puchnarewicz E. M., Harnden F. R., 1992, ApJS, 81, 66
De Zotti G., Gaskell C. M., 1985, A&A, 147, 1
Elvis M., Lockman F. J., Wilkes B. J., 1989, AJ, 97, 777
Ferland G. J., Persson S. E., 1989, ApJ, 347, 656
Fiore F., Elvis M., Mathur S., Wilkes B., McDowell J., 1993, ApJ, 415, 129
Gaskell C. M., 1985, ApJ, 291, 112
Gaskell C.M., 1987, in Kundt W., ed., Astrophysical Jets and their Engines. Reidel, Dordrecht, p. 29
Gaskell C. M., Koratkar A. P., 1996, ApJ, in press
Gezari D. Y., Schmitz M., Mead J. M., 1987, Catalog of Infrared Observations. NASA Reference Publication 1196

Grandi S. A., 1981, ApJ, 251, 451
Grandi S. A., Osterbrock D. E., 1978, ApJ, 220, 783
Green A. R., McHardy I., Lehto H. J., 1993, MNRAS, 265, 664
Halpern J. P., Oke J.B., 1987, ApJ, 312, 91
Hamann F., Ferland G. J., 1993, ApJ, 418, 11
Hartig G. F., Baldwin J. A., 1986, ApJ, 302, 64
Joly M., 1987, A&A, 184, 33
Joly M., 1991, A&A, 242, 49
Joly M., 1993, Ann. Phys. Fr., 18, 241
Laor A., Fiore F., Elvis M., Wilkes B. J., Mcdowell J., 1994, ApJ, 435, 611
Lawrence A., Papadakis I., 1993, ApJ, 414, L85
Lawrence A., Ward M. J., Elvis M., Fabbiano G., Willner S., Carleton N. P., Longmore A., 1985, ApJ, 291, 117
Lawrence A., Saunders W., Rowan-Robinson M., Crawford J., Ellis R. S., Frensk C. S., Efstathiou G., Kaiser N., 1988, MNRAS, 235, 261
Lipari S., 1994, ApJ, 436, 102
Lipari S., Macchetto F. D., Golombek D., 1991, ApJ, 366, L65
Lipari S., Terlevich R., Machetto F., 1993, ApJ, 406, 451
Lipari S., Colina L., Machetto F., 1994, ApJ, 427, 174
Low F.J., Cutri R.M., Kleinmann S. G., Huchra J. P., 1989, ApJ, 340, L1
Mathur S., Wilkes B., Elvis M., Fiore F., 1994, ApJ, 434, 493
Murphy E. M., Lockman F. J., Laor A., Elvis M., 1996, ApJS, 105, 369
Netzer H., 1985, ApJ, 289, 451
Norman C., Miley G., 1984, A&A, 141, 85
Osterbrock D.E., 1977, ApJ, 325, 733
Pfefferman E. et al., 1987, Proc. SPIE, 733, 519
Puchnarewicz E. M., Mason K. O., Cordova F.A., Kartje J., Branduardi-Raymont G., Mittaz J. P. D., Murdin P. G., Allington-Smith J., 1992, MNRAS, 256, 589
Rigopoulou D. A., Lawrence A., Rowan-Robinson M., 1996, MNRAS, 278, 1049
Trümper J., 1983, Adv. Space. Res., 4, 21
Véron-Cetty M. P., Véron P., 1989, A Catalogue of Quasars and Active Nuclei. ESO Report No. 7 (VCV)
Weymann R. J., Morris S. L., Foltz C. B., Hewett P. C., 1991, ApJ, 373, 23
Wilkes B. J., Elvis M., McHardy I., 1987, ApJ, 321, L23
Wills B., 1982, in Heeschen D.S., Wade C.M., eds, Proc. IAU Symp. 97, Extragalactic Radio Sources. Reidel, Dordrecht, p. 373
Zheng W., Keel W. C., 1991, ApJ, 382, 121
Zheng W., O'Brien P. T., 1990, ApJ, 353, 433